Sensorless Control of an SPMSM drive using a second-order Sliding Mode Observer

Barna Temesi

Abstract—This short design documentation presents the used system model, parameters and rotor position estimator. The acquired structure is called Sensorless control of a PMSM using an SMO. The used observer is of second-order. Gain calculation strategies are also presented.

Index Terms: dynamic modelling of syncronous motors, Super-twisting Algorithm, PMSM, Sensorless control, Sliding Mode Observer, b-EMF voltage observer

1 INTRODUCTION

As in every design process, after the problem statement, the system has to be modeled and analyzed. This starts with an overview of the motor parameters. Next, the motor voltage equations, which are already given in the dq-reference frame, are examined. The mechanical equation of the motor is also presented.

This documentation does not consider the FOC used in the system. The focus is strictly on the rotor position estimator.

2 MODEL OF THE SYSTEM

The motor, in the scope of this thesis, is an SPMSM. This means that the permanent magnets are located on the surface of the rotor. Due to this, the motor is non-salient, and also the reluctance path is equal on the d- and q-axis. This results in equal inductance on the d- and q-axis. For easier understanding, the machine inductance will be denoted as L_s [2].

$$L_d = L_q = L_s \tag{1}$$

The most important parameters of the motor and the other necessary system parameters are listed in the table 1.
As can be seen from the table, the motor has 4 pole pairs. Generally speaking, this means that the machine is more geared towards high-speed operation. In high-torque operation applications, like in the case of a steering motor, the number of poles might exceed a 100.
In simulations, the total system resistance will be used, which takes into account the resistance of every possible component in the setup [1].

Table 1: *System parameters, from previous projects such as*

Description	Notation	Value	Unit
Number of pole pairs	N_{pp}	4	-
Winding resistance	R_w	0.19	Ω
Total system resistance	R_s	0.268	Ω
q and d-axis inductance	L_m	2.2	mH
Rotor PM flux linkage	λ_{mpm}	0.12258	wB
Rated speed, SPMSM	$\omega_{m,rated}$	4500	rpm
Rated torque, SPMSM	$\tau_{m,rated}$	20	Nm
Rated power, SPMSM	$P_{m,rated}$	9.4	kW
Rated speed, IM	$\omega_{IM,rated}$	1400	rpm
Rated torque, IM	$\tau_{IM,rated}$	14	Nm
Rated power, IM	$P_{IM,rated}$	2.2	kW
Rated current, VSI	I_{VSI}	35	A
IM machine inertia	J_{IM}	0.0069	$kg \cdot m^2$
SPMSM machine inertia	J_{SPMSM}	0.0048	$kg \cdot m^2$
Total system inertia	J_{sys}	0.0146	$kg \cdot m^2$
Coulomb friction	C	0.2295	Nm
Viscous friction	B	0.0016655	N

The motor voltage equations are shown in equation (2). Due to the assumption that the system is symmetrical and balanced, the zero term (v_0) is zero.

$$\begin{aligned} v_d &= R_s i_d + p\lambda_d - \omega_r \lambda_q \\ v_q &= R_s i_q + p\lambda_q + \omega_r \lambda_d \\ v_0 &= 0 \end{aligned} \tag{2}$$

In the abc-reference frame, the machine flux-linkage is dependent on position and the machine inductance is constant for a non-salient pole machine, but because the model is already transformed into the $dq0$-reference frame, the machine inductance is constant.

The stator $dq0$-reference frame is aligned with the rotor reference frame, which is naturally in the $dq0$-reference frame. The rotor d-axis is chosen to be aligned with the maximum flux density line at no load condition. The q-axis is always leading the d-axis by 90 degrees electric. This way, it is aligned with the minimum flux density line [1].

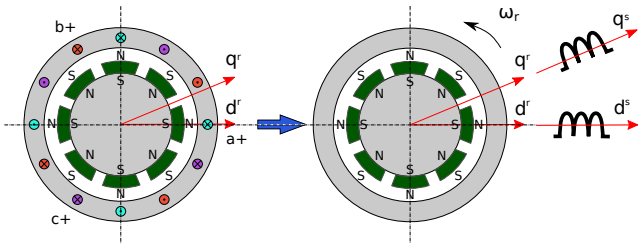

Figure 1: *Reference frame transformation from* ***abc*** *to dq. The structure of the motor is also shown. Inspiration: [3]*

The two d-axis is in line now. This is convenient because, it results in the d-axis and the q-axis flux-linkage as shown in equation (3).

$$\begin{aligned} \lambda_d &= (L_{ls} + L_{md})\, i_d + \lambda_{mpm} = L_d i_d + \lambda_{mpm} \\ \lambda_q &= (L_{ls} + L_{mq}) = L_q i_q \\ \lambda_0 &= 0 \end{aligned} \tag{3}$$

After substitution, the voltage equations may be rewritten as seen in equation (4).

$$\begin{aligned} v_d &= R_s i_d + p(L_d i_d + \lambda_{mpm}) - \omega_r L_q i_q \\ v_q &= R_s i_q + p(L_q i_q) + \omega_r (L_d i_d + \lambda_{mpm}) \end{aligned} \tag{4}$$

Where p is the differential operator $\frac{d}{dt}$. Differentiating the equation, keeping in mind that the derivative of a constant is zero, will result in the following.

$$\begin{aligned} v_d &= R_s i_d + L_d p i_d - \omega_r L_q i_q \\ v_q &= R_s i_q + L_q p i_q + \omega_r (L_d i_d + \lambda_{mpm}) \end{aligned} \tag{5}$$

In one more step, the homogeneous first-order differential equation of the system is acquired.

$$\begin{aligned} \frac{d}{dt} i_d &= -\frac{R_s}{L_d} i_d + \frac{1}{L_d} v_d + \omega_r \frac{L_q}{L_d} i_q \\ \frac{d}{dt} i_q &= -\frac{R_s}{L_q} i_q + \frac{1}{L_q} v_q - \omega_r \frac{L_d}{L_q} i_d - \frac{1}{L_q} \omega_r \lambda_{mpm} \end{aligned} \tag{6}$$

Equations (4) also contain the back-EMF voltage components which are very important in position estimation, hence they are highlighted here:

$$\begin{aligned} e_d &= -\omega_r L_q i_q \\ e_q &= \omega_r (L_d i_d + \lambda_{mpm}) \end{aligned} \tag{7}$$

The governing torque equation can be derived from the equation of the input power of the windings. Simplifying this equation, using the attributions of the SPMSM machine, yields the following expression:

$$T_e = \frac{3}{2} N_{pp} \left(\lambda_d i_q - \lambda_q i_d\right) \tag{8}$$

$$T_e = \frac{3}{2} \frac{N_{poles}}{2} (\lambda_{mpm} i_q + (L_d - L_q) i_d i_q) \tag{9}$$

$$T_e = \frac{3}{2} N_{pp} \left(\lambda_{mpm} i_q\right) \tag{10}$$

Using Newton's second law, the mechanical equation of the system can be derived as shown in equation (11) [1].

$$T_e = J \frac{d\omega_m}{dt} + B_m \omega_m + T_{dist} \tag{11}$$

Where J is the total system inertia and T_{dist}, the disturbance torque, consists of the load torque and Coulomb friction. The total system inertia includes the inertia of both the IM and PMSM machine and also the coupling and fastening components between them.

The first term is related to the torque needed to accelerate the system without friction, the last two terms are related to the torque which is needed to overcome the viscous friction and the disturbance torque, respectively.

3 Rotor Position Estimation

The goal of this estimator is to estimate the b-EMF voltages in $\alpha\beta$ reference frame and then calculate the rotor position from it. The rotor speed can also be acquired by a simple integration of the rotor position state. The implemented estimator is a sliding mode observer. The theory behind non-linear observer can be found in: [4]. The design is based on [1].

The modified structure of the system, now including the observers, is presented in figure 2.

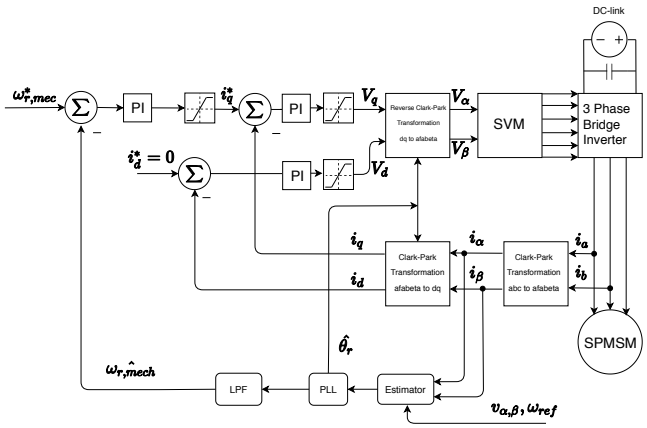

Figure 2: *Structure of control system with a generalized estimator included*

4 Second-Order Sliding Mode Observer

A system using a traditional, first-order sliding mode observer needs multiple filters to deal with the chattering problem present in the observer output signal. This increases the overall complexity of the system [6].

Implementing a higher-order sliding mode observer, for instance, a super twisting observer (STO), instead, is a popular way of reducing the number of filters needed in a system [6].

The order of the observer is increased by introducing new terms that are then integrated into the observer law. The main characteristic of a higher-order sliding mode observer is that the observer signal is now made continuous. Furthermore, it allows for a sliding mode on $\sigma = \dot{\sigma} = 0$ using only σ [5]. In this case, σ is defined the same as for the first-order SMO, $\boldsymbol{\sigma} = \hat{\boldsymbol{i}}_{\boldsymbol{s}} - \boldsymbol{i}_{\boldsymbol{s}}$, due to the fact that the system remained the same.

Using the same starting point for the design, as for the first-order sliding mode observer, the traditional super-twisting observer law is formulated in equations (12), (13).

$$\begin{aligned} \frac{d\hat{i}_\alpha}{dt} &= f\hat{i}_\alpha + gu_\alpha + gk_1\sqrt{|\ \sigma_\alpha\ |}sign(\sigma_\alpha) + gw_\alpha \\ \frac{d\hat{i}_\beta}{dt} &= f\hat{i}_\beta + gu_\beta + gk_1\sqrt{|\ \sigma_\beta\ |}sign(\sigma_\beta) + gw_\beta \end{aligned} \tag{12}$$

$$\begin{aligned} \dot{w}_\alpha &= k_2 sign(\sigma_\alpha) \\ \dot{w}_\beta &= k_2 sign(\sigma_\beta) \end{aligned} \tag{13}$$

Where $f = -\frac{R_s}{L_s}, g = \frac{1}{L_s}$, and the errors, $\sigma_\alpha = \hat{i}_\alpha - i_\alpha, \sigma_\beta = \hat{i}_\beta - i_\beta$.

The first observer gain (k_1) corresponds to the dynamic performance of the observer, and the second gain (k_2) is responsible for smoothing out the output signal. The smoothing is done by integration of the sign function. Before looking at the proof of the stability, it can be seen that k_2 has to be larger than k_1 to attenuate the chattering, but the ratio cannot be too high because that would reduce the overall performance of the system in transients.

It is preferred to use a slightly modified form of this observer. The $\sqrt{|\ \sigma_{\alpha,\beta}\ |}$ term is omitted. In fact, this is the algorithm that is implemented in the attached model. This new observer law is shown in equations (14), (15).

$$\begin{aligned} \frac{d\hat{i}_\alpha}{dt} &= f\hat{i}_\alpha + gu_\alpha + gk_1 sign(\sigma_\alpha) + gw_\alpha \\ \frac{d\hat{i}_\beta}{dt} &= f\hat{i}_\beta + gu_\beta + gk_1 sign(\sigma_\beta) + gw_\beta \end{aligned} \tag{14}$$

$$\begin{aligned} \dot{w}_\alpha &= k_2 sign(\sigma_\alpha) \\ \dot{w}_\beta &= k_2 sign(\sigma_\beta) \end{aligned} \tag{15}$$

The two terms with the observer gains in equation (12) directly give the estimated back-EMF signal, as presented in equation (16).

$$\begin{aligned} \hat{e}_\alpha &= -k_1\sqrt{|\ \sigma_\alpha\ |}sign(\sigma_\alpha) - \int \dot{w}_\alpha dt \\ \hat{e}_\alpha &= -k_1\sqrt{|\ \sigma_\beta\ |}sign(\sigma_\beta) - \int \dot{w}_\beta dt \end{aligned} \tag{16}$$

4.1 Observer gain calculation

It can be noticed that in an SPMSM, the perturbation terms are the following:

$$\begin{aligned} \rho_{1,\alpha} &= fi_\alpha + gu_\alpha \\ \rho_{1,\beta} &= fi_\beta + gu_\beta \end{aligned} \tag{17}$$

In other words, the perturbation terms are the terms present in equation (12) but not in equation (16).
The stability of the observer is shown in details in [1]. For this system, it is a fair assumption that the first perturbation term is globally bounded, such as:
$|\ \rho_1\ | \leq \delta_1\sqrt{|\ max(e_\alpha, e_\beta)\ |}$
Also, there is no second term present in this system, hence:
$\rho_2 = 0$.
If this is true, the expressions for the gains can be simplified, as show in equation (18).

$$\begin{aligned} k_1 &> 2\delta_1 \\ k_2 &> k_1\frac{5\delta_1 k_1 + 4\delta_1^2}{2(k_1 - 2\delta_1)} \end{aligned} \tag{18}$$

Where δ_1 is a positive constant. From the above equation (18), it can be seen that many gain combinations will result in a stable system because there is not an explicit equation or an upper constraint defined for the gains. It is worth repeating it here, that higher observer gains will result in higher chattering, so a practical upper bound may be set. This formula implies the necessity of experimental tuning of the observer.

Another approach to finding the observer gains is presented in [5]. This is an explicit strategy for choosing the parameters. The gains are chosen based on the measure of the perturbation in the system. The condition, that the perturbations have to be bounded, must be true again.

$$\begin{aligned} k_1 &= 1.5\sqrt{max(\rho_{1,\alpha}, \rho_{1,\beta})}, \\ k_2 &= 1.1max(\rho_{1,\alpha}, \rho_{1,\beta}) \end{aligned} \tag{19}$$

Equation (19) defines a nonlinear relation between the gains. The detailed proof for this case is not shown in this report, but it can be found in [5].

The approach presented above is generally not used in SPMSM applications because the gains are chosen non-linearly. It can be expected, from the first-order sliding mode observer, that using static observer gains is not feasible here, because the perturbation terms, equation (17), can change in a wide range.

As a conclusion, the observer gains will be tuned later in both simulation and the laboratory according to a linear law, based on the reference speed, or they will be changed using a look-up table, based on experimental results.

5 Conclusion

For further information, simulation results, experimental data, please check [1].

References

[1] B. Temesi, U. G. Gautadottir, *Sensorless Control of PMSM Drive Using Sliding-Mode-Observers* AAU, Denmark, 2020 Master's thesis.

[2] D. Wilson, *Motor Control Compendium*, 1st-ed . 2011

[3] K. Lu, *Control of Electrical Drive Systems and Converts Lecture 1 Slides*, 1st-ed . pp. 1-30, 2019

[4] J. E. Slotine, W. Li, *Applied Nonlinear Control* Englewood Cliffs, New Jersey: Prentice Hall, 1991.

[5] Y. Shtessel, C. Edwards, L. Fridman, and A. Levant, *Sliding Mode Control and Observation* 1st. edition, Birkhäuser Basel, 2014, p. 356, ISBN: 978-0-8176-4892-3. DOI:10.1007/978-0-8176-4893-0.

[6] D. Liang, J. Li, and R. Qu, *Super-twisting algorithm based sliding-mode observer with online parameter estimation for sensorless control of permanent magnet synchronous machine* ECCE 2016 - IEEE Energy Conversion Congress and Exposition, Proceedings, pp. 1–8, 2016. DOI: 10.1109/ECCE.2016.7855479